3D Bioprinter + Electrospinner for Bone-Ligament Tissue Engineering

Sherif H. Aboubakr, MS[*†]; Steven Nery, BS[*‡]; Lauren Long, BS[*]; Christopher A. Buksa, BS[*§]; Chanju Fritch, BS[¶]; Christina Salas, PhD[*§\\]

[*]Department of Orthopaedics & Rehabilitation, The University of New Mexico Health Sciences Center, Albuquerque, New Mexico

[†]Department of Civil Engineering, The University of New Mexico, Albuquerque, New Mexico

[‡]Department of Electrical Engineering, The University of New Mexico, Albuquerque, New Mexico

[§]Department of Mechanical Engineering, The University of New Mexico, Albuquerque, New Mexico

[¶]School of Medicine, The University of New Mexico Health Sciences Center, Albuquerque, New Mexico

[\\]Center for Biomedical Engineering, The University of New Mexico, Albuquerque, New Mexico

Abstract

Modern 3D bioprinters have been shown to allow for precise control of structural geometry to build patient-specific scaffolds for tissue regeneration—primarily non-load-bearing tissue. However, 3D bioprinting is limited by cell viability, polymer cross-linking characteristics, and poor tensile properties. In comparison, electrospinning has been used to form fibrous structures with accelerated cellular maturation properties, improved growth and migration of cells, and increased tensile properties. Conversely, the mostly uncontrolled deposition of electrospun fibers can limit pore size and cell infiltration. In our Orthopaedic Biomechanics & Biomaterials Laboratory, a custom 3D Bioprinter + Electrospinner hybrid system (E-Spin Printer) was designed to merge the positive aspects of both technologies to allow for hierarchical, functionally-graded scaffolds with high load-bearing characteristics. This hybrid system was made from open-source components and is customizable to meet the accuracy, resolution, and repeatability of high-end bioprinters and electrospinners, at a cost of less than $10,000. We introduce this technology and provide a broad description of one application for its use.

Introduction

3D bioprinting can be defined as the printing of biopolymer and high-concentration cell solutions. Typically, 10 to 1000 μm resolution is required to form tissue-like structures, with higher-viscosity materials often providing structural support for the printed structure and lower-viscosity materials providing a suitable environment for maintaining cell viability and function. Laboratories across the world have designed and created 3D bioprinters to fabricate replacement human-scale tissues and organs, often with structural integrity and biological function similar to native tissues. These printed structures have been shown to be stable and amenable to revascularization, making them ideal for application in replacement of injured tissue. At this time, few bioprinter systems have been targeted toward fabricating tissue with high tensile and compressive strength requirements.

The main steps in the 3D bioprinting process are imaging and digital design, selection of materials and cells, and printing of the scaffolds.[1-6] Imaging such as computed tomography (CT) and magnetic resonance imaging (MRI) are essential to replicate the complex, heterogeneous architecture of functional tissues. Further segmentation, surface rendering, and stereolithographic editing can provide a full volumetric description of the specific tissue examined. Computer-aided design and computer-aided manufacturing (CAD-CAM) tools and mathematical modeling techniques can then be used to collect and digitize the complex tomographic and architectural information. This is followed by deposition and patterning of materials in successive layers as directed by the CAD-CAM software, wherein each deposited layer serves as a foundation for the following layers until the 3D structure is patterned and completed (Figure 1A). Inkjet, micro-extrusion, and laser-assisted printing can all be used for deposition and patterning tissue materials.[1-6]

The electrospinning fabrication technique uses high voltage (5 to 30 kV) to create an electric field between a droplet of polymer solution (typically at the tip of a syringe needle) and a metallic collector plate (Figure 1B). The main

forces acting on the polymer droplet are the electrostatic field and the electrostatic repulsion of charges. These forces are opposed by the surface tension of the droplet, and the viscoelastic forces of polymer. When electrostatic repulsion charges exceed the surface tension, stretching (ie, elongating at very high strain rates) of the polymer droplet occurs, and a continuous fiber is ejected toward the collector plate. Polymer solution viscosity, surface tension, electrical conductivity, and dielectric constant are key parameters for the electrospinning process controllable by solution selection and optimization. Applied voltage, flow rate of solution, collector material properties, diameter of the needle, and distance between applicator and collector are other key parameters of the electrospinning process controllable by hardware setup, selection, and design. Temperature, humidity, and pressure should also be considered.[7,8]

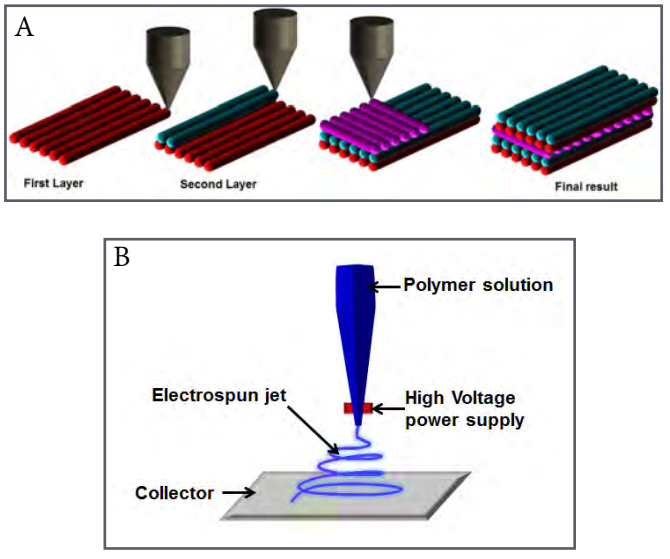

Figure 1. (A) Representative example of 3D bioprinting using multiple bioinks deposited from their respective syringe deposition systems. (B) Representative schematic describing the primary characteristics of an electrospinner.

Traditionally, electrospinning processes have control over microstructural porosity, density, and tensile strength while lacking macroscale geometric control. Porosity and density control has been shown to enable cellular migration, elongation, and proliferation needed for differentiation of mesenchymal stem cells to ligament fibroblasts. The tensile strength characteristics will enable properties closer to that of native ligament than other biomanufacturing techniques. Electrospinner characteristics contrast to those of the 3D-bioprinting process that allows for geometric control but lacks a process to vary microstructural properties. Shortcomings of 3D bioprinting are especially limiting when tissues must be attached to bone; the materials that contain properties amenable to extrusion and cellular viability do not adhere to rigid structures without considerable material modifications. The geometric control allowed by 3D printing will enable patient-specific reproductions of the hard and regeneration of soft tissue. The cost of isolated electrospinners ranges from $25,000 to $50,000 with electrospray capabilities. Entry-level 3D bioprinters commercially range from $75,000 to $500,000 with multiple nozzles and additional features for polymerization of materials.

We introduce the development of a low-cost, modular 3D Bioprinter + Electrospinner hybrid system (E-Spin Printer) for targeted fabrication of scaffolds of the bone, ligament, and bone-ligament interface. This system aims to merge the positive aspects of each technology. We present a summary of the developed technology and describe an application for its use. All fabrication and experimental validation was completed our Orthopaedic Biomechanics & Biomaterials Laboratory.

Design

The design of our technology is presented henceforth. It is important to note that while we describe specific materials used in development of the first prototype, the design is universal such that similar materials from different manufacturers may serve the same purpose.

Stepper Motor Controller

The printer is controlled by a Smoothieboard 5x, a low cost (< $200), open source stepper motor controller with flexible software configuration (Uberclock, Gold Hill, OR). The controller runs five stepper motors simultaneously, with up to 2.5 amps of current when powered with a 24-volt power supply. Our printer uses five motors in its current design: three for X, Y, Z motion and two to drive custom syringe pumps (one for printer, one for electrospinner). The other inputs of the Smoothieboard could also run several cooling fans and multiple heated beds, and the inputs are compatible with most open-source software. The controller was chosen for its flexible hardware and software configurations and extensive online documentation. As additional print heads or other items are added to the system, it may be necessary to add a larger controller or additional controllers to handle the added components.

Linear Stages

For X, Y, and Z axis movement, we purchased several Newmark eTrack linear stages for their specified resolution,

accuracy and repeatability (Newmark Systems Inc, Rancho Santa Margarita, CA). Each stage was fitted with a NEMA 17 stepper motor rated at 1.2 amps. The leadscrew configuration of the linear stages allows for more precise movement over belt-driven stages at the cost of speed. The X stage is 300-mm long, whereas the Y and Z stages are 200 mm and 150 mm, respectively. The X stage enables positioning of the build plate under the 3D bioprinter or electrospinner deposition heads, respectively. The Y stage is mounted orthogonally to the X stage for front-to-back plate positioning. The Z axis is vertically mounted to the frame of the printer, allowing for height control of the print nozzle. Newmark rails range from $782 (50 mm) to $962 (300 mm). The selected rails have a 0.24-mm resolution, an accuracy of 0.0006 mm/mm, and a max speed of 150 mm/s. Figure 2 shows the X, Y, and Z rails mounted in the frame of the E-Spin Printer.

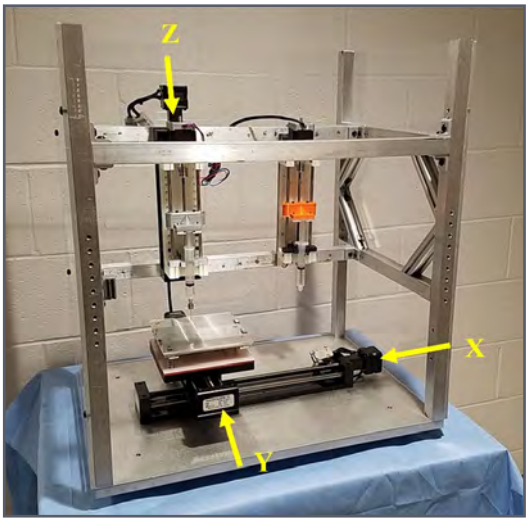

Figure 2. Early embodiment of our E-Spin Printer hybrid system. X, Y, and Z linear stages are noted with arrows showing axis of travel.

Print Bed

The custom print bed was designed as a surface for printed material and an electrical conductor for the electrospinner of the system. The print bed is a layered system of acrylonitrile-butadiene-styrene (known as ABS) plastic, rubber, nylon, aluminum, and glass supported by three leveling screws (Figure 3). The aluminum layer is machined to allow insertion of a 4- by 6-inch heated polychlorinated-biphenyl (PCB) bed. To help reduce unwanted conductivity from the electrified print bed during electrospinning, a 1-inch air gap was designed between the print bed and Y-linear stage. Additionally, the print bed is attached to the linear stage using nylon screws to further reduce unwanted electrical charge throughout the system.

Figure 3. Close-up view of an early embodiment of our hybrid system showing the build plate (asterisk), bioprinter syringe pump (left arrow), and electrospinner syringe pump (right arrow).

Syringe Pumps

The extrusion system consists of two custom syringe pumps that were constructed using 3D-printed nylon and off-the-shelf hardware (Figure 3). The design borrows and improves on the open-source OpenPump system and is one of the most cost-effective ways to create a syringe pump. To reduce torsion during syringe deposition, the end-mounts were redesigned to attach directly to a custom base plate that fixed to the Z axis of the printer frame. The fixture that holds the syringe plunger was modified to allow easy access to slide bearings and improve grip on the plunger of the syringe during deposition. Each pump was fitted with a NEMA 17 stepper motor controlled by the Smoothieboard. The hardware consists of an M5 threaded rod, M8 smooth rods, couplers and slide bearings.

Electrospinner

The electrospinner consists of a steel syringe tip, the aluminum plate of the print bed, and a low-cost ($250) 5- to 30-kV variable high-voltage power supply purchased from Information Unlimited (Amherst, NH). The power supply was chosen for its low cost and safety features, specifically, a current limiting feature to reduce risk of shock or injury, which lowers amperage to safe levels (700 μA at 35 kV). In operation, the negative lead of the power supply clamps directly to the aluminum plate of the build plate, and the positive lead connects directly to the steel needle of the mounted syringe. As voltage is increased, an electric field is created between the syringe needle and print bed. Solution exiting the syringe becomes charged and quickly collects on the glass surface of the negatively-

charged build plate (Figure 4).

Our system also includes a modification to allow for aligned fiber spinning. For this, the negative lead is replaced by two negative leads, each is connected to a single extruded metal bar positioned on either side of the desired print surface, near the target area. The negative leads are triggered in an alternating fashion to direct flow of the solution exiting the syringe, back and forth depending on the activated lead.

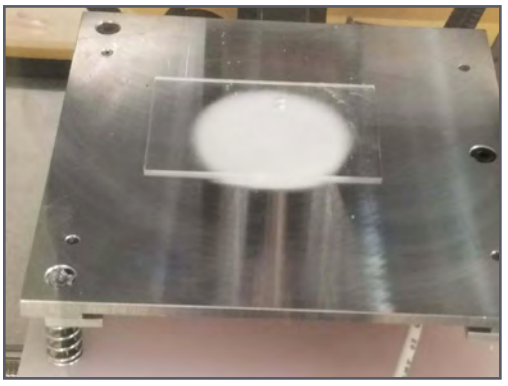

Figure 4. Close-up view of electrospun fiber deposition on build-plate (white). Note the white lead at the bottom that provides a negative charge to the plate.

3D-Modeling Software

All initial 3D modeling was created using OpenSCAD, an open-source CAD program. The program was free under the General Public License and allowed for rapid modeling and stereolithography file exporting. When moving toward patient-specific modeling of hard and soft-tissue scaffolds, we will use Mimics (Materialise, Leuven, Belgium) CT and MRI to 3D-modeling software and MedCad (Dallas, TX) for integrating the scaffolds with surrounding hard tissue. A flowchart of the planned steps for fabrication are shown in Figure 5. In short, a torn ligament would be identified through CT or MRI (A). The data can be exported to a medical imaging software to develop a 3D model of the bone and insertion points (B). The software can be used to simulate native tissue replacement. Solid files can be exported and read by the E-Spin Printer and converted to G-code for fabrication (C). The scaffold is built and cells are seeded for growth (D). The scaffold can be immediately implanted into a patient, or the tissue can be grown fully before implantation (E).

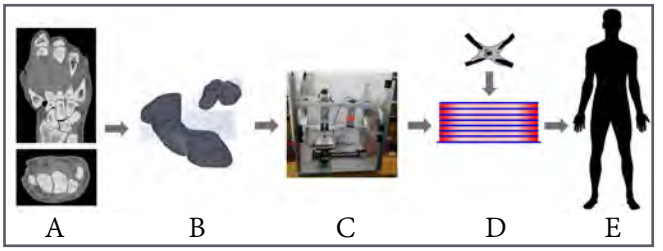

Figure 5. Flowchart showing representative process for moving from computed tomography and magnetic resonance imaging (MRI) to implantation.

Slicing Software

Our printer currently uses the open-source program Slic3r to generate G-code for construction. Slic3r was chosen because, with some code modification, it allows the user to assign extruders (ie, syringe pumps) to each material to be printed or spun. This feature was exploited to allow our machine to alternate between our syringe pumps (each holding different materials). By exploiting this feature, we are also able to create a gradient between materials in all directions (X, Y, Z). More on material deposition is described in subsequent sections. Currently, popular open-source 3D slicing software is not optimized for bioprinting. Future embodiments of our technology will require advanced customization of the Slic3r software to allow for use of three or more bioinks and electrospun filament.

Potential Fabrication Materials

3D bioprinter—synthetic and natural bioinks. Alginate was chosen as a suitable hydrogel to validate our 3D-bioprinting technology. An alginate-based bioink was printed, and hydroxyapatite (HAp) bioceramic particles were added to enhance mechanical properties to ensure a functionally graded bone-ligament interface transition. Notably, alginate requires mixture with calcium ions for polymerization. Thus, this material may not be suitable for use in mammals owing to calcium ion leaching that would surely occur. Thus polyethylene (glycol) diacrylate (known as PEG-DA) with a photoinitiator has been selected as a new printing material to control viscosity by addition of exfoliated clay[9] or HAp nanoparticles. Note that the current design is not limited to any polymer type, but some polymers may require implementation of additional materials or hardware to aid in polymerization. e.g. A photoinitiator and UV lighting system may be required for polymerization. It is important to also note that cells can be included in the composition of the bioink. The cell-infused bioink is transported via syringe pumps through the system. When cells are included, further optimization of the syringe pump control will be needed to maintain

cellular viability. Additionally, we are working with a collaborator for printing of cell-encapsulating proteins that would aid in direct-cell printing.

Electrospinner—synthetic and natural polymers. Polycaprolactone (PCL) was chosen as a primary test material because it has been shown to be a suitable, biocompatible polymer for electrospinning.[10,11] However, collagen will be used in future iterations because of its function as a component of extracellular matrix (ECM) in connective tissues.[12] This makes it a more suitable choice for electrospun connective-tissue scaffolds. Collagen fiber alignment is essential for scaffold architecture and mechanical properties. Moreover, the use of collagen fiber diameter has been critical in the design of scaffolds because it is deterministic of scaffold mechanical properties, cell proliferation, matrix production, and differentiation regulation.[13]

Application

As a first application of our technology, we aim to print a patient-specific bone-ligament scaffold for regeneration of the scapholunate ligament.

Problem

The scapholunate ligament has been identified as the most commonly injured hand ligament by the American Society for Surgery of the Hand.[14] Ligament healing is not common owing to a reduced number of cells and blood vessels that exist in and around the soft tissue. Healing, usually in partial tears of the ligament, is often a result of scar-tissue formation. For full ligament ruptures, the most common surgical treatment is ligament reconstruction, usually with a tendon harvested from the upper extremity. Unfortunately, autographs have been shown to cause donor-site morbidity and do not match the mechanical properties of the native tissue. Therefore, orthopaedic-related research has focused on strategies to improve and accelerate the healing process through tissue-engineered scaffolds.[15-18]

Notable Considerations in Tissue Engineering

When designing and assessing a scaffold for use in tissue engineering, the following six factors should be considered: 1) Biocompatibilty: scaffolds should be biocompatible for cells to adhere, function, and migrate onto the surface and through the scaffold. Scaffold implantation must evoke a negligible immune reaction to prevent any excessive inflammatory responses. 2) Biodegradability: scaffolds are not intended to be a permanent implants and should eventually be replaced by native tissue. The scaffold degradation byproducts should not be cytotoxic. 3) Mechanical properties: scaffolds should have mechanical properties (ie, strength and stiffness) consistent with the anatomical site into which it is to be implanted. Moreover, scaffolds should be practically strong enough to allow for manual manipulation during surgical procedures. 4) Mechanical integrity: scaffolds should have sufficient mechanical integrity to function from the time of implantation to completion of the remodeling process of native tissue. 5) Scaffold architecture: scaffolds should accommodate cellular penetration and adequate diffusion of nutrients and waste products to and from cells. 6) Fabrication technology: scaffolds should be cost effective and patient specific to be commercially and clinically viable.[1,18]

Scaffold Fabrication Process

The introduced E-Spin Printer system allows for a functionally-graded (laterally), alternating layer (vertically) deposition method. The novelty of our technology, using a single X-Y rail system underlying the 3D bioprinter and electrospinner syringe pumps, respectively, allows for this unique deposition method. The functionally-graded characteristic will allow a gradual transition, horizontally, from the bone phase to ligament phase then back to bone phase using bioinks from multiple syringes—each with a varying concentration of HAp nanoparticles and other necessary material modifiers. The bulk scaffolds will vary vertically made from alternating layers of PEGDA-based bioink (or other) and PCL (collagen, or other) electrospun fibers (Figure 6).

The bioinks will be tuned to serve as a viable ECM environment to support cell migration, growth, and proliferation. To aid in this, some bioinks will be fabricated from decellularized human tissue such that the ECM environment is maintained to support desired cellular activity. The electrospun fibers will be tuned to support high tensile loads such as those experienced by the native ligament; these fibers provide most of the mechanical stability and strength of the bulk scaffold. Multiscale material and structural optimization will be required to control microstructure, mechanical properties, and biodegradation rates of the scaffold.

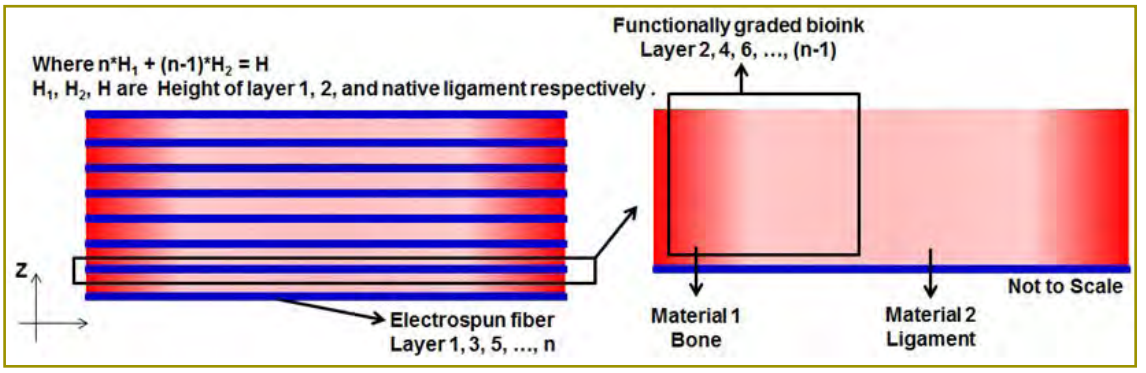

Figure 6. Schematic representation of the (Left) hierarchical and (Right) functionally-graded composite scaffold targeted with this technology.

Conclusion

The current article introduces our custom E-Spin Printer hybrid system and provides broad details on one application for this new technology. This system combines state-of-the-art digital composite fabrication tools of 3D-bioprinting and electrospinning to target fabrication of hierarchical, 3D scaffolds for regeneration of bone, ligament, and the bone-ligament transition region. By starting with the scapholunate ligament to validate our technology, this hybrid system has broad and notable application in all areas of tissue engineering, particularly those areas with high tensile (ie, ligaments and tendons) and compressive (ie, meniscus and cartilage) load-sustaining requirements. The 3D printing aspect of the system will further allow for targeted implantation and customization for tissue replacement at any anatomical region. Furthermore, the open-source, modular nature of our hybrid technology was achieved at a cost less than $10,000—which was nearly $100,000 less than any commercially-available 3D bioprinter with the same capabilities—and $15,000 less than the least expensive electrospinner.

Funding

The authors received support from a basic science research grant from the American Foundation for Surgery of the Hand and a faculty-development award from Advance@UNM, a National Science Foundation (NSF)-funded project at The University of New Mexico (UNM). Additional financial support was provided by UNM Department of Orthopaedics & Rehabilitation.

Conflict of Interest

The authors report no conflicts of interest.

Acknowledgments

Special thanks to Dr. Mahmoud Reda Taha and Dr. Nick Carroll in The University of New Mexico Department of Civil Engineering and Department of Chemical and Biological Engineering, respectively, for their cooperation and support.

References

1. O'brien FJ. Biomaterials & scaffolds for tissue engineering. Mater Today (Kidlington);14(3):88-95. doi: 10.1016/S1369-7021(11)70058-X.
2. Murphy SV, Atala A. 3D bioprinting of tissues and organs. Nat Biotechnol 2014;32(8):773-85. doi: 10.1038/nbt.2958.
3. Zhu W, Ma X, Gou M, Mei D, Zhang K, Chen S. 3D printing of functional biomaterials for tissue engineering. Curr Opin Biotechnol 2016;40:103-12. doi: 10.1016/j.copbio.2016.03.014.
4. Dodziuk H. Applications of 3D printing in healthcare. Kardiochir Torakochirurgia Pol 2016;13(3):283-293.
5. Zhang X, Zhang Y. Tissue engineering applications of three-dimensional bioprinting. Cell Biochem Biophys 2015;72(3):777-82. doi: 10.1007/s12013-015-0531-x.
6. Hölzl K, Lin S, Tytgat L, Van Vlierberghe S, Gu L, Ovsianikov A. Bioink properties before, during and after 3D bioprinting. Biofabrication 2016;8(3):032002.
7. Teo WE, Ramakrishna S. A review on electrospinning design and nanofiber assemblies. Nanotechnology 2006;17(14):R89-R106. doi: 10.1088/0957-4484/17/14/R01.
8. Reneker DH, Yarin AL. Electrospinning jets and polymer nanofibers. Polym 2008:49(10):2387-425.
9. Hong S, Sycks D, Chan HF, et al. 3D printing of highly stretchable and tough hydrogels into complex, cellularized structures. Adv Mater 2015;27(27):4035-40. doi:
10. Croisier F, Duwez AS, Jérôme C, et al. Mechanical testing of electrospun PCL fibers. Acta Biomater 2012;8(1):218-24. doi: 10.1016/j.actbio.2011.08.015.

11. Kang X, Xie Y, Powell HM, et al. Adipogenesis of murine embryonic stem cells in a three-dimensional culture systemusing electrospun polymer scaffolds. Biomaterials 2007;28(3):450-8.
12. Mienaltowski MJ, Birk DE. Structure, physiology, and biochemistry of collagens. Adv Exp Med Biol 2014;802:5-29. doi: 10.1007/978-94-007-7893-1_2.
13. Erisken C, Zhang X, Moffat KL, Levine WN, Lu HH. Scaffold fiber diameter regulates human tendon fibroblast growth and differentiation. Tissue Eng Part A 2013;19(3-4):519-28. doi: 10.1089/ten.tea.2012.0072.
14. Wolfe SW. Scapholunate instability. J Am Soc Surg Hand 2001;1(1):45-60. doi: 10.1002/adma.201501099.
15. Hogan MV, Kawakami Y, Murawski CD, Fu FH. Tissue engineering of ligaments for reconstructive surgery. Arthroscopy 2015;31(5):971-9. doi: 10.1016/j.arthro.2014.11.026.
16: Yilgor C, Yilgor Huri P, Huri G. Tissue engineering strategies in ligament regeneration. Stem Cells Int 2012;2012:374676. doi: 10.1155/2012/374676.
17: Sapir-Lekhovitser Y, Rotenberg MY, Jopp J, Friedman G, Polyak B, Cohen S. Magnetically actuated tissue engineered scaffold: insights into mechanism of physical stimulation. Nanoscale 2016;8(6):3386-99. doi: 10.1039/c5nr05500h.
18: Rodrigues MT, Reis RL, Gomes ME. Engineering tendon and ligament tissues: present developments towards successful clinical products. J Tissue Eng Regen Med 2013;7(9):673-86. doi: 10.1002/term.1459.